TRB Annual Meeting

A Conservative Car Following Model Based on Adverse Weather Conditions

--Manuscript Draft--

Full Title:	A Conservative Car Following Model Based on Adverse Weather Conditions
Abstract:	This study investigates the integration of traditional car-following models with machine learning techniques to analyze car-following behavior in the presence of lane-changing interactions on multi-lane road segments. Traditional car-following models, such as the Intelligent Driver Model (IDM), are effective with limited data and robust to noise but often fail to capture complex driving behaviors. In contrast, data-driven models like Gaussian Process Regression (GPR) can model intricate behaviors but require extensive, high-quality datasets. To leverage the strengths of both approaches, we propose a hybrid framework that combines IDM with GPR, using IDM as a prior to enhance GPR predictions. The analysis demonstrates that the hybrid model significantly improves the accuracy of acceleration predictions compared to IDM alone, effectively capturing the nuances of real-world driving scenarios. This approach mitigates the limitations of traditional models and reduces the dependency on large datasets. The findings underscore the potential of combining traditional and data-driven methods to improve traffic behavior simulations, offering promising applications in traffic management and autonomous driving. Future research will focus on extending this framework to other driving behaviors and integrating additional data sources for further enhancement.
Additional Information:	
Question	**Response**
The total word count limit is 7500 words including tables. Each table equals 250 words and must be included in your count. Papers exceeding the word limit may be rejected. My word count is:	6995
Manuscript Classifications:	Operations; Traffic Simulation ACP80; Calibration/Validation; Car-following; Vehicle Trajectory
Manuscript Number:	TRBAM-25-04255
Article Type:	Presentation
Order of Authors:	Kaitai Yang
	Yuan-Zheng Lei
	Yi Zhang
	Xianfeng Yang

A CONSERVATIVE CAR FOLLOWING MODEL BASED ON ADVERSE WEATHER CONDITIONS

Kaitai Yang
Ph.D. Candidate & Graduate Research Assistant
Department of Civil and Environmental Engineering
University of Maryland, College Park, MD, U.S., 20742
Email: kaitai74@umd.edu

Yuan-Zheng Lei
Ph.D. Candidate & Graduate Research Assistant
Department of Civil and Environmental Engineering
University of Maryland, College Park, MD, U.S., 20742
Email: yzlei@umd.edu

Yi Zhang
Ph.D. Candidate & Graduate Research Assistant
Department of Civil and Environmental Engineering
University of Maryland, College Park, MD, U.S., 20742
Email: zhangyi@umd.edu

Xianfeng Terry Yang, Ph.D., Corresponding Author
Associate Professor
Department of Civil and Environmental Engineering
University of Maryland, College Park, MD, U.S., 20742
Email: xtyang@umd.edu

Word Count: 6245 words + 3 table(s) × 250 = 6995 words

Submission Date: August 1, 2024

ABSTRACT
Car-following model is fundamental in transportation engineering and traffic flow theory, providing critical insights into vehicle-level dynamics and interactions. Traditional models typically assume idealized weather conditions and often neglect the impacts of adverse weather on driving behaviors, leading to inaccurate modeling under varied environmental conditions. To address these shortcomings, this study extends the classical Intelligent Driver Model (IDM) by integrating a novel term, namely the Conservative Intelligent Driver Model (CIDM), to further capture drivers' conservative behaviors on slippery roads during snowy and rainy days. This enhancement adjusts the desired following distance, allowing the model to reflect real-world driver reactions to reduced visibility and decreased road friction more accurately. Comprehensive stability analysis and criteria derivation confirm the model's robustness and the CIDM's efficacy is evaluated using real-world vehicle trajectory data under both rainy and snowy conditions. The results demonstrate that the developed CIDM not only enhances the robustness of parameter estimates under critical conditions but also maintains accuracy, significantly improving the reliability of the model in diverse environmental settings. This study highlights the CIDM's potential as a superior alternative to traditional car-following models, enhancing traffic safety and efficiency through more accurate and reliable behavior prediction models, especially in adverse weather scenarios.
Keywords: Car-following model, Microscopic simulation

INTRODUCTION

Car-following models, integral components in the domain of transportation engineering and traffic flow theory, warrant a comprehensive understanding to address complex traffic dynamics (*1*). Serving as microscopic representations of traffic interactions, these models illuminate the driver's responses when following a preceding vehicle within the same lane. Grounded in the fundamental principles of motion, car-following models usually posit a correlation between a vehicle's acceleration and various attributes, including its current speed, the gap with the preceding vehicle, and the relative speed difference. The key to car-following theory lies in the stimulus-response framework ((*2*); (*3*)), which suggests that a driver's response (acceleration) is influenced by the immediate driving environment (stimulus) and their personal sensitivity. Various models have adopted different factors, both external and internal, to serve as stimuli in order to simulate the responses that determine acceleration patterns. These models generally rely on a generic equation that connects key factors of vehicle behavior, as illustrated below:

$$dv_n(t) = f(v_n, s_n(t), \Delta v_n(t), \ldots)dt \quad (1)$$

Here, the nth vehicle's acceleration at time step t is related to its current state of speed v, space gap s and speed difference Δv with its leading vehicle, and so on. Utilizing car-following models facilitates the analysis of traffic flow dynamics at the individual vehicle level, offering a comprehensive overview of various influencing factors and conditions. Additionally, these models act as a crucial bridge between individual behaviors and macroscopic analysis. By transforming micro-level behaviors into macro-level outcomes, these models empower researchers and traffic management authorities to comprehend better, anticipate, and manage traffic flow, thereby enhancing transportation systems.

A significant assumption within classical car-following models is the premise of ideal environmental conditions, specifically, consistently ideal weather. Such assumptions may lead to undesirable performance when the ambient driving environment changes, given that car-following behavior inherently involves the integration of the driver, vehicle, and environment ((*4*)). On the other hand, employing data-driven methods to investigate car-following behavior under adverse weather conditions (especially rain and snow) appears unfeasible. This is because, to the best knowledge of the authors, currently available open-source vehicle trajectory data are mainly collected under good weather conditions. Additionally, the presence of rain and snow may complicate video recording (for example, snow may cover the camera) and trajectory extraction, making the collection of a large dataset unfeasible. Recognizing the impact the adverse weather, numerous studies have been conducted to investigate the impacts of weather changes. The most significant influences are the reduction in visibility and the decrease in road adhesion. (*5*) assessed the impact of fog on stable driving, acceleration, and deceleration stages, respectively. Through questionnaires, (*6*) found that drivers tend to adopt more conservative driving behaviors when visibility is low. (*7*) developed a modified FVDM to describe drivers' car-following behavior under varying levels of visibility. In addition to reduced visibility, adverse weather conditions can also lead to decreased road adhesion. (*8*) calibrated the Wiedemann car-following model using field data, suggesting that drivers tend to maintain lower acceleration rates and velocities while keeping a larger vehicle headway under snowy conditions. (*9*) calibrated the Van Aerde car-following model using field data collected from icy roads in Hokkaido, highlighting significant statistical differences in response time, desired velocity, velocity, road capacity, and congestion density.

To enhance the understanding of car-following behavior under inclement weather conditions, simple calibration of classical car-following models may not suffice, as these models typically overlook the influence of weather in their formulations. Furthermore, existing research has predominantly explored the effects of reduced visibility and compromised tire-road adhesion in isolation. Therefore, the development of a modified classical car-following model, informed by real-world datasets gathered under adverse weather conditions, presents a promising avenue. The objective of this study is to propose a model that is not only able to accurately simulate drivers' behaviors but also provides insights into the adjustments necessitated by such conditions. In light of the gaps identified and the goals of this research, this study leverages the Intelligent Drive Model(IDM) as the base model due to its accurate simulation capabilities and clear explanation of each parameter (*10*). This paper first seeks to examine the limitations of the IDM under adverse weather conditions, followed by proposing a modified version of the IDM to rectify the issue. Subsequently, real-world data collected under both rainy and snowy weather conditions are adopted to investigate the performance of the proposed model.

The remainder of the paper is organized as follows: Section 2 introduces the proposed methodology; Section 3 demonstrates the performance of the proposed model using real-world data collected under rainy and snowy weather conditions; and finally, Section 4 concludes with a discussion on the proposed model and suggestions for future work.

METHODOLOGY

Review of the Intelligent Driver Model

The original IDM can be expressed as follows:

$$\frac{dv_n}{dt} = a[1 - (\frac{v_n}{v_0})^{\delta} - (\frac{s^*(v_n, \Delta v_n)}{s_n})^2] \tag{2}$$

The free accelerating term $a[1 - (\frac{v_n}{v_0})^{\delta}]$, governs the acceleration of the vehicle. Here, a represents the maximum acceleration, and v_0 denotes the vehicle's desired speed. Given an unobstructed path for a stationary vehicle, the vehicle would first accelerate at the rate of a, and the acceleration gradually decreases as the speed increases. Such reduction is controlled by the exponent term δ, and the vehicle would not exceed its desired speed. In accordance with the IDM author's recommendation (*11*), this paper assigns the value of 4 to δ.

$$s^*(v_n, \Delta v_n) = s_0 + max(v_n T + \frac{v_n \Delta v_n}{2\sqrt{ab}}, 0) \tag{3}$$

$$\Delta v_n = v_n - v_{n-1} \tag{4}$$

$$S_n = x_{n-1} - l_{n-1} - x_n \tag{5}$$

On the other hand, the vehicle's decelerating process is regulated by the braking term $(\frac{s^*(v_n, \Delta v_n)}{s_n})^2$, where $s^*(v_n, \Delta v_n)$ represents vehicle's desired gap and s_n is the actual gap as shown by Equations 3 - 5. The term $s_0 + v_n T$ denotes the vehicle's desired following distance at the steady state. Here, the minimum gap, s_0, represents the space gap between the standstill vehicles, T is the time gap that the driver aims to maintain while in motion. The dynamic term $\frac{v_n \Delta v_n}{2\sqrt{ab}}$, symbolizes the driver's response to the speed difference Δv_n based on its own comfortable deceleration b. One of the merits of IDM is its flexibility in representing various driving styles by altering parameter values.

When weather conditions shift from normal to adverse, the two most evident changes involve the reduction in visibility and the decrease in road adhesion. The reduction in visibility may increase the driver's estimation error and reaction time, leading to changes in driving behaviors. However, research has shown that such impacts could be compensated for by the driver's spatial and temporal anticipation. Additionally, classical car-following models have demonstrated good performance even without accounting for these specific human errors (*12*). Although adverse weather conditions can constrain the maximum acceleration and deceleration capabilities, drivers rarely utilize these full capacities in actual driving scenarios. Incorporating terms directly related to such environmental changes can be challenging due to the difficulty in precisely measuring and quantifying factors such as visibility and tire-road friction. Moreover, the IDM effectively captures driver characteristics, with each parameter representing a distinct driver trait rather than a physical-world feature. Therefore, developing a modified IDM by introducing a parameter that denotes changes in a driver's level of caution in response to decreased visibility and road adhesion during adverse weather conditions appears more reasonable.

The IDM employs distinct terms to represent acceleration and deceleration patterns, reflecting the different actions a driver may take during different following patterns. This study first investigates the IDM's capacity to represent acceleration and deceleration independently. During adverse weather conditions, drivers typically adopt more cautious behavior, maintaining slower speeds, reducing acceleration rates, and preferring to keep larger distances from the vehicle ahead (*13*). As previously mentioned, the IDM portrays accelerating behavior as a smooth and continuously decreasing action as speed increases, well defined by the parameters v_0 and a. This cautionary behavior during acceleration can be symbolized by reducing these parameters' values. Simultaneously, increasing the values of T and s_0 could depict the desire for a greater following distance at a steady state. One instinctive method to illustrate an increase in caution as the following vehicle approaches the leading one (i.e., when $\Delta v_n > 0$) is to change the value of b. However, unlike a, merely changing the value of b does not necessarily lead to good performance in deceleration. As a result, such modification may not accurately reflect the cautious behavior and might even negatively impact the model's performance. The physical interpretation of the parameter b is "comfortable deceleration", and the magnitude of b determines not only the deceleration rate but also significantly influence the driver's braking strategy. Generally, a driver with a lower b value tends to accept a lower deceleration rate when feeling safe and might even engage in more abrupt braking compared to a driver with a higher comfortable deceleration rate during critical scenarios (*14*). To illustrate, consider a situation where a vehicle is in a driving condition with a following distance $s_n = s_0 + v_n T$, and the leading vehicle suddenly reduces its speed to zero.

The braking term calculates the deceleration rate is shown as follows:

$$-a\left(\frac{s_n+\frac{v_n^2}{2\sqrt{ab}}}{s_n}\right)^2 = -\frac{v_n^2\sqrt{ab}}{bs_n} - a - \frac{v_n^4}{ans_n^2} \tag{6}$$

With the kinematic deceleration rate:

$$b_{kin} = \frac{v_n^2}{2s_n} \tag{7}$$

$$-a\left(\frac{s_n+\frac{v_n^2}{2\sqrt{ab}}}{s_n}\right)^2 = -\frac{2b_{kin}\sqrt{ab}}{b} - a - \frac{b_{kin}^2}{b} \tag{8}$$

As articulated in Equation 8, when $\Delta v_n > 0$, the driver's deceleration behavior is directly related to the relationship between b_{kin} and b. If $b_{kin} \geq b$, the driver interprets this as a critical condition, thereby opting for a larger deceleration than deemed necessary. Conversely, if $b_{kin} < b$, the driver would perceive the scenario as non-critical and thereby opt for a deceleration less than b and will brake harder and harder as b_{kin} increases.

To illustrate this behavior, a simulation was conducted, maintaining all the other parameters at their recommended values. Drivers operating vehicles at a speed of $54km/h$, but possessing different values of b, would exhibit significantly different maneuvers under the same circumstances. As depicted in Figure 1, at the start of the simulation, a driver with $b = 1m/s^2$, perceives the scenario as critical and thus applies a deceleration much greater than the comfortable deceleration rate. Conversely, a driver with $b = 2.5m/s^2$ perceives the situation as safe and initially applies only a minor deceleration, subsequently braking more intensively until the comfortable deceleration rate is reached. While the driver with $b = 1.5m/s^2$ exhibits a braking behavior that falls between that of the drivers with $b = 1m/s^2$ and $b = 2.5m/s^2$, reaching the maximum deceleration rate at a similar time to the driver with $b = 1m/s^2$ and achieving a maximum deceleration rate comparable to that of the driver with $b = 2.5m/s^2$. Generally, the maximum value of b should not be greater than the acceleration due to gravity. By keeping all other parameters constant, an extremely conservative driver with $b = 0.6m/s^2$ could generate a similar deceleration rate to an extremely aggressive driver with $b = 9.8m/s^2$. The primary difference is when they reach the maximum deceleration rate. Neither an extremely small nor a large value of b is desirable for conducting simulation as they may both generate an unreasonably large deceleration rate.

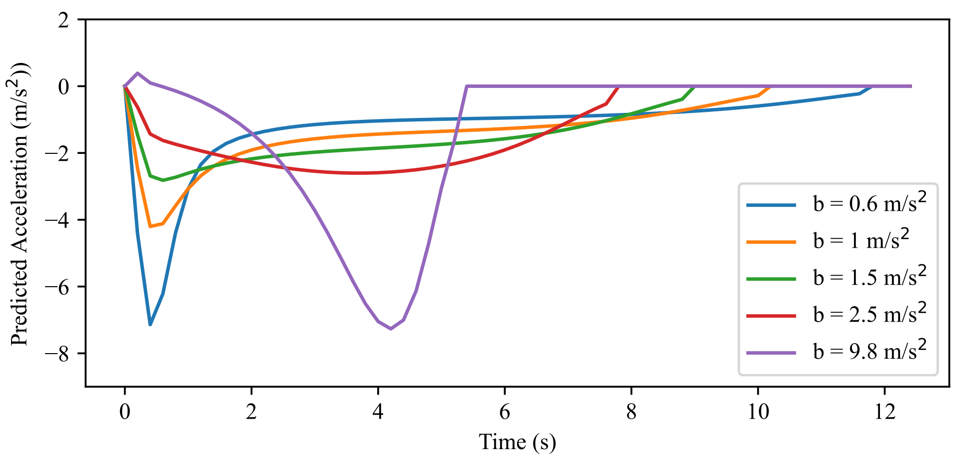

FIGURE 1: Illustration of the variations in braking behaviors among drivers with different b values

Further elucidation is provided in Figure 2, which display the predicted acceleration rates when following a vehicle traveling at a constant speed of 80km/h. These figures depict how drivers with differing values of s_n and Δv_n would respond. Notably, the red and the dashed lines represent the contour lines of predicted acceleration equal to $0m/s^2$ and $-7m/s^2$, respectively, the region with predicted acceleration smaller than $-7m/s^2$ is regarded as unrealistic in reality considering the reduction of the road tire adhesion due to the inclement weather conditions. It can be shown that a driver with a smaller comfortable deceleration rate is more sensitive than those with a larger comfortable deceleration rate. This phenomenon can be directly observed by examining the dynamic term $(v_n \Delta v_n)/(2\sqrt{ab})$. Under the same circumstances, a smaller b can lead to a larger desired gap, thus causing harder braking.

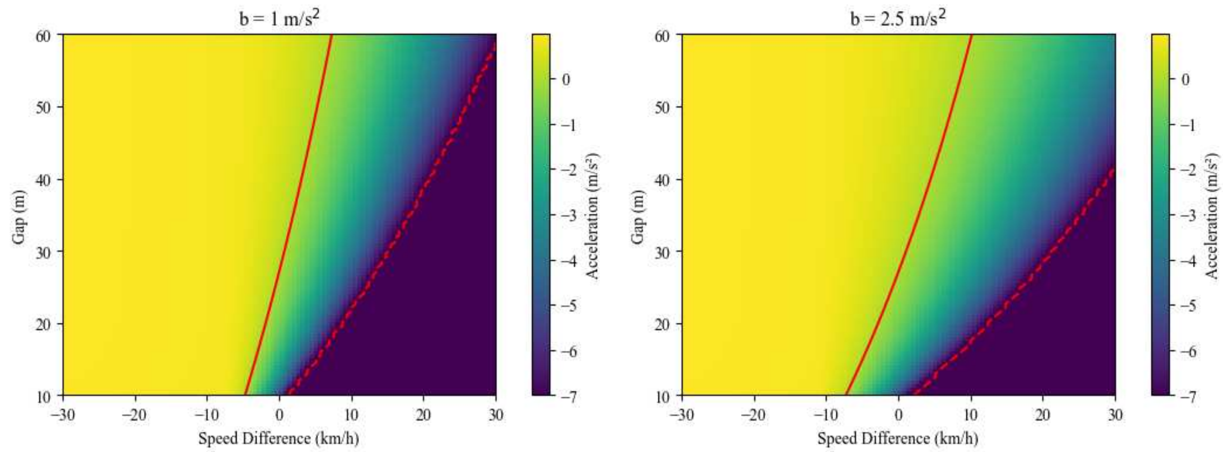

(a) feasible deceleration regions for $b = 1m/s^2$ (b) feasible deceleration regions for $b = 2.5m/s^2$

FIGURE 2: Illustration of the feasible deceleration regions for drivers with different b values

Conservative Intelligent Driver Model under adverse weather condition

As previously mentioned, the magnitude of b plays a crucial role in influencing driver behavior, especially in response to the leading vehicle decelerating. This parameter not only dictates the maximum deceleration rate achievable but also the timing at which this maximum rate is attained. Drivers characterized by a lower b value exhibit more conservative driving patterns under perceived safe conditions yet may tend to overreact in critical conditions. Conversely, individuals with a higher b value display greater resilience in critical scenarios but tend to behave more aggressively. Therefore, solely adjusting the magnitude of b cannot accurately capture such conservative behavior under adverse weather conditions. Therefore, introducing a parameter representing the driver's conservative level due to the inclement weather conditions seems promising. In this study, "conservative" refers to the driver's increased tolerance for a larger following distance to the leading vehicle and heightened sensitivity to a decrease in this distance under adverse weather conditions, as compared to normal weather. This approach assumes that, despite reduced visibility, drivers can still detect deceleration in the leading vehicle through brake lights, and acknowledge that it will take a larger distance to brake due to reduced tire-road friction in adverse conditions. Conversely, the delayed recognition of the leading vehicle's acceleration by the following vehicle may result from reduced visibility, a more cautious driving approach, or diminished vehicular acceleration performance on slippery roads. Regarding the sensitivity of a driver's braking behavior as it relates to the value of b, and to make the proposed model as parsimonious as possible, this study introduces an additional term into the desired gap equation. This term directly accommodates the driver's response to the speed difference in adverse weather conditions, as expressed in Equation 9:

$$s^*(v_n, \Delta v_n) = s_0 + max(v_n T + \frac{R^2}{2}\log(1 + (\frac{max(\Delta v_n, -k)}{R})^2) + \frac{v_n \Delta v_n}{2\sqrt{ab}}, 0) \tag{9}$$

Preserving the original definitions of the parameters in accordance with the IDM, this study introduces an additional parameter, denoted as R. R is a positive parameter representing the increase in the desired gap under adverse weather conditions compared to normal conditions. Rather than attributing such conservative behavior solely to changes in the parameter b during the approach phase, this study considers such behavior as an increase in the desired following distance, reflecting a heightened level of driver caution. The newly added $\frac{R^2}{2}\log(1+(\frac{max(\Delta v_n,-k)}{R})^2)$ is enlightened by an adaptive robust kernel function (*15*), which ensures that the driver will initiate a more substantial deceleration when the product of $v_n \Delta v_n$ is relatively small (i.e., safe condition). However, when this product is sufficiently large, $\frac{v_n \Delta v_n}{2\sqrt{ab}}$ will dominate the desired gap, prompting the driver to decelerate at a rate similar to that observed in the original IDM. It's important to note that the newly introduced term also assumes a positive value, offsetting the negative $v_n \Delta v_n$, to reflect the driver's tolerance for an increased following distance or reduced friction resulting in a slower acceleration rate. Additionally, the term $max(\Delta v_n, -k)$ ensures that, when the leading vehicle significantly outpaces the following one, the following vehicle will still adopt the maximum acceleration rate as the negative impact of $v_n \Delta v_n$ becoming greater than the compensatory added term, in this study, k is set to -4 m/s. Such benefits are illustrated in Figure 3. Given the same $\Delta v_n = 3m/s$, drivers exhibit distinct behaviors depending on the value of v_n. The proposed model, named the Conservative Intelligent Driver Model (CIDM) shows that drivers brake more forcefully when $v_n \Delta v_n$ is low and perform in a manner similar to the predicted behavior predicted by the original IDM with a b value of 1.4 as $v_n \Delta v_n$ increases.

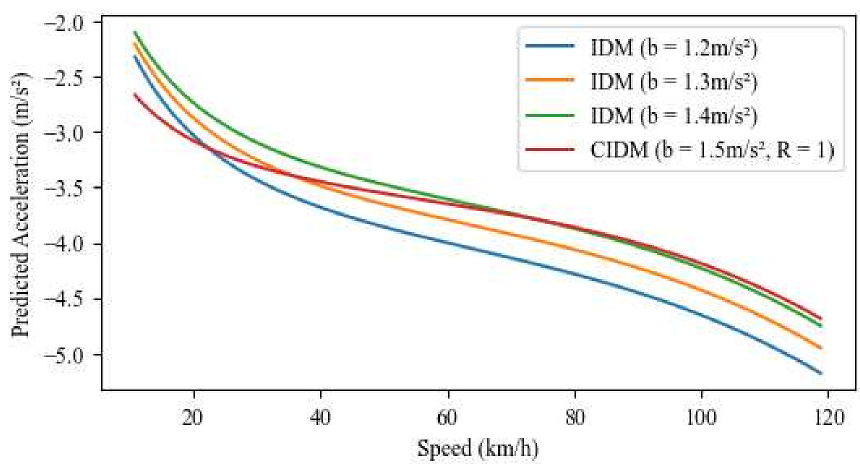

FIGURE 3: Comparison of predicted deceleration by IDM and CIDM

It should be noted that the newly introduced term affects the desired following distance only in the presence of a speed difference, indicating that the vehicle's free acceleration and behavior at equilibrium would remain consistent with the original IDM. However, when there is a nonzero speed difference, a limitation of the added term is that R cannot take a value of zero, ensuring that this term remains positive whenever a speed difference is present. The purpose of introducing this term is to enable the modeling of potential conservative driving behavior. If this behavior can be accurately calibrated from field data, the modified model's performance should be at least equivalent to that of the original IDM. In other words, the addition of this term is not intended to compromise the IDM's performance, nor is it assumed that conservative behavior is always present.

To evaluate whether the added term might detrimentally affect model performance, a simulation was conducted, the results of which are displayed in Figure 4. When R is set to 0.1, even if the speed difference reaches 120km/h, the impact of the newly added term to the desired following distance is negligible. Therefore, it is suggested that during calibration, if the value of R is calibrated to be 0.1 or less, the modified model can be considered equivalent to the original IDM in terms of performance. This conclusion is further supported by experimental findings.

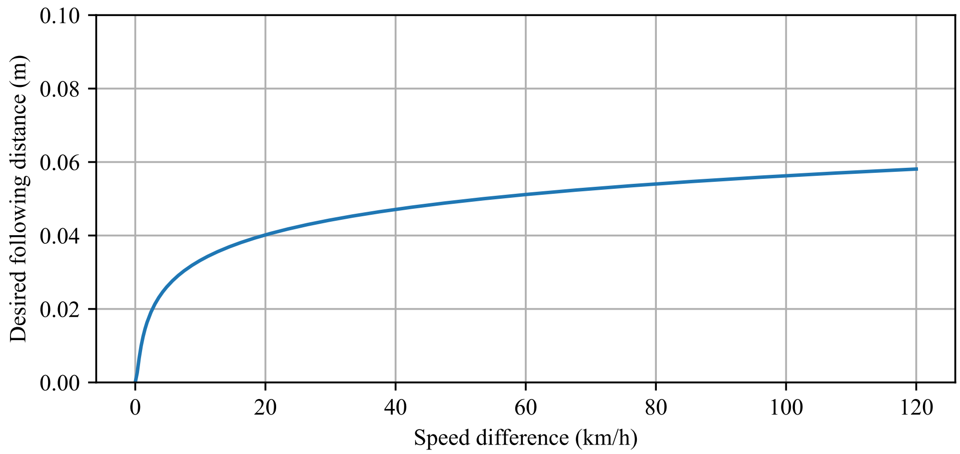

FIGURE 4: Illustration of the impact of speed difference to the desired following distance when $R = 0.1$

EXPERIMENTAL STUDY

Case setup and data collection

Several key questions require resolution: (1) What constitutes an effective calibration method for the proposed model? (2) Will the CIDM yield parameters akin to those of the IDM? (3) Under what circumstances does CIDM become the same as the IDM? To evaluate the proposed model's efficacy and address these questions, this study used two real-world vehicle trajectory datasets collected separately under rainy and snowy weather conditions. The rainy dataset is provided by the CitySim dataset (*16*). CitySim is a cutting-edge vehicle trajectory dataset that extracts vehicle trajectory data from high-resolution videos recorded by drones at various locations. As shown in Figure 5, this study uses the Expressway-A dataset collected from a weaving segment located in Asia. The snowy dataset was collected by the author at the I-695 highway segment in Baltimore, Maryland, United States on 01/15/2024 using a drone, in total 50 minutes video was collected and transformed into the vehicle's trajectory. The car-following pairs were identified based on each vehicle's coordinates at the same time step.

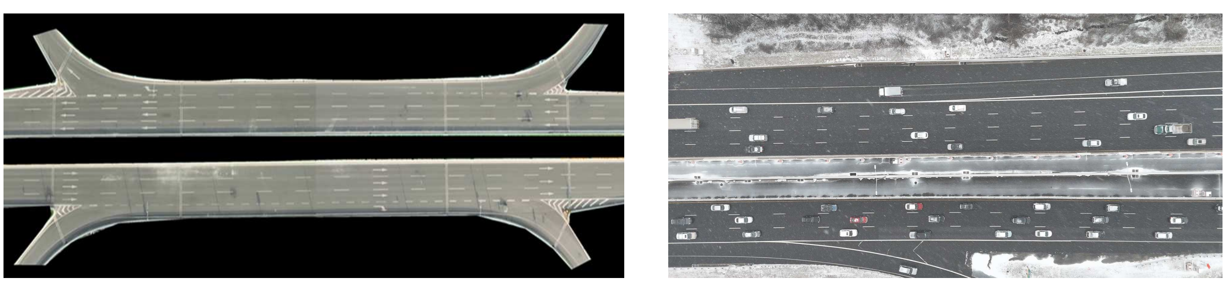

(a) Stretch of rainy weather dataset segment (b) Stretch of snowy weather dataset segment

FIGURE 5: Illustration of target road segments

To address the influence of lane-changing behavior on car-following behavior, and considering the variation in individual driving styles, this study aims to evaluate the performance of the CIDM and IDM using individual vehicle trajectories. The calibration objective is to identify an optimal parameter set that minimizes the discrepancy between the car-following behaviors predicted by the model and those observed in reality. Calibration of a car-following model involves choosing an appropriate optimization algorithm, a goodness-of-fit (GoF) function, and a measure of performance (MoP). In this study, the Genetic Algorithm (GA) is chosen for parameter calibration due to the complexity of the models. GA, a heuristic nonlinear optimization algorithm inspired by biological evolution, has proven to be an effective and reasonable method for calibrating various car-following models ((*17*), (*14*), (*18*), (*19*)). Furthermore, the combination of MoP and GoF can significantly influence the effectiveness of the calibration process. As shown by Equations 10 – 11, this study investigates the two most commonly used combinations for calibration: the root mean square error (RMSE) of speed ((*20*), (*21*), (*22*)), and RMSE of spacing ((*23*), (*24*), (*25*)). A lower GoF value indicates a more precise simulation.

$$RMSE(v) = \sqrt{\frac{1}{T}\sum_{t=1}^{T}[v_i(t) - \widetilde{v}_i(t)]^2} \tag{10}$$

$$RMSE(s) = \sqrt{\frac{1}{T}\sum_{t=1}^{T}[s_i(t) - \widetilde{s}_i(t)]^2} \tag{11}$$

$$v_n(t+\Delta t) = v_n + a_n(t)\cdot\Delta t \tag{12}$$

$$x_n(t+\Delta t) = x_n(t) + \frac{v_n(t)+v_n(t+\Delta t)}{2}\cdot\Delta t \tag{13}$$

where $v_i(t)$ and $s_i(t)$ represent the observed speed and spacing of the ith vehicle at time t, respectively, and $\widetilde{v}_i(t)$ and $\widetilde{s}_i(t)$ correspond to the simulated speed and spacing.

To ensure that the calibrated parameters of the CIDM and IDM remain within a realistic range, their boundaries are defined as follows: The time gap T is set between [0.1, 3] seconds and the minimum spacing s_0 is limited to [1, 5] meters. The maximum acceleration is restricted to [0.1, 4] m/s^2, which correlates with a maximum acceleration rate of 4 m/s^2 (equivalent to 0-100km/h in 6 seconds), while the comfortable deceleration boundary is set at [0.1, 9] m/s^2. The parameter R is bounded within [0.01, 15]. The upper limit of the desired velocity v_0 is set to 33.6 m/s (120km/h). Regarding the lower limit, it should be noted that this limit must exceed the highest velocity value observed in the dataset, a detail often overlooked in other studies. This is a critical consideration because if the actual velocity exceeds v_0, the power of 4 applied in the $(\frac{v_n}{v_0})^4$ can induce an excessively large deceleration. It is important to remember that v_0 in the IDM is primarily designed for modeling acceleration and is not intended to handle deceleration scenarios (*11*). In this study, the parameters for executing the GA for calibration are as follows: the GA will run for a maximum of 500 generations, with each generation consisting of a population of 200. The mutation rate is set to 0.05. Additionally, this study employs a ballistic integration scheme, as detailed in Equations 12 and 13. This scheme utilizes an integration time step, Δt, of 0.2 seconds, which is used for the periodic updating of vehicle speed and position. For the sake of computing intensity, the sampling rate employed in this study is 0.2s for both datasets, which has been deemed sufficient for calibrating the car-following model (*26*).

In addition, it should be noted that aside from calibration settings, the quality of data can significantly impact the calibration results when a single trajectory is used to emulate driving behaviors. The effectiveness of a training dataset depends more on its quality than on its sheer volume (*26*). A trajectory that includes only a stop-and-go scenario is insufficient for calibrating the desired speed, as it lacks the corresponding condition. Therefore, verifying the dataset's completeness is a crucial step before calibration. Considering that the proposed model primarily focuses on investigating driver's behavior to the speed difference under rainy and snowy weather conditions, trajectories from seven vehicles, all containing deceleration regimes, are selected for calibration. These are calibrated using RMSE(s) and RMSE(v) as separate objective functions.

Results discussions

Case study 1: rainy weather conditions

TABLE 1: Calibration Results of IDM and CIDM with RMSE(s) of rainy dataset

Vehicle	v_0	T	s_0	a	b	R	RMSE(s)	RMSE(v)
358 (IDM)	11.02 m/s	1.54 s	3.27 m	3.98 m/s^2	1.28 m/s^2	NA	0.733	0.332
358 (CIDM)	11.72 m/s	1.53s	3.25 m	3.93 m/s^2	2.50 m/s^2	1.16	0.726	0.331
730 (IDM)	27.16 m/s	0.95 s	2.25 m	0.87 m/s^2	0.18 m/s^2	NA	0.507	0.400
730 (CIDM)	15.24 m/s	1.54 s	2.03 m	2.47 m/s^2	6.13 m/s^2	10.87	0.417	0.409
1340 (IDM)	7.50 m/s	1.15 s	2.41 m	2.55 m/s^2	8.82 m/s^2	NA	0.858	0.437
1340 (CIDM)	7.50 m/s	1.13 s	2.42 m	2.58 m/s^2	8.84 m/s^2	0.08	0.854	0.440
1814 (IDM)	9.93 m/s	0.50 s	2.63 m	3.97 m/s^2	0.10 m/s^2	NA	0.482	0.306
1814 (CIDM)	9.93 m/s	0.50 s	2.56 m	3.93 m/s^2	0.10 m/s^2	3.39	0.477	0.300
4231 (IDM)	13.26 m/s	1.17 s	2.73 m	2.43 m/s^2	0.73 m/s^2	NA	0.625	0.483
4231 (CIDM)	14.18 m/s	1.18 s	2.71 m	2.53 m/s^2	0.87 m/s^2	0.04	0.625	0.479
5283 (IDM)	19.76 m/s	1.29 s	3.95 m	0.68 m/s^2	0.59 m/s^2	NA	0.431	0.475
5283 (CIDM)	18.33 m/s	1.06 s	3.92 m	0.72 m/s^2	1.01 m/s^2	2.91	0.421	0.474

TABLE 2: Calibration Results of IDM and CIDM with RMSE(v) of rainy dataset

Vehicle	v_0	T	s_0	a	b	R	RMSE(s)	RMSE(v)
358 (IDM)	32.95 m/s	1.97 s	1.66 m	0.66 m/s^2	1.94 m/s^2	NA	1.578	0.226
358 (CIDM)	29.10 m/s	1.95 s	1.68 m	0.65 m/s^2	1.92 m/s^2	0.07	1.582	0.226
730 (IDM)	30.34 m/s	1.28 s	2.70 m	0.83 m/s^2	0.24 m/s^2	NA	1.117	0.377
730 (CIDM)	31.41 m/s	1.87 s	1.88 m	2.00 m/s^2	2.43 m/s^2	8.30	0.764	0.363
1340 (IDM)	31.61 m/s	1.19 s	1.89 m	1.29 m/s^2	9.00 m/s^2	NA	1.212	0.319
1340 (CIDM)	31.04 m/s	1.17 s	1.75 m	1.35 m/s^2	8.99 m/s^2	0.56	1.277	0.316
1814 (IDM)	32.96 m/s	0.81 s	3.30 m	3.31 m/s^2	8.99 m/s^2	NA	1.366	0.229
1814 (CIDM)	30.36 m/s	0.78 s	3.43 m	3.58 m/s^2	8.97 m/s^2	0.75	1.422	0.221
4231 (IDM)	11.78 m/s	1.34 s	3.31 m	1.96 m/s^2	7.19 m/s^2	NA	1.854	0.323
4231 (CIDM)	12.01 m/s	1.34 s	3.30 m	2.00 m/s^2	7.91 m/s^2	0.02	1.848	0.323
5283 (IDM)	19.36 m/s	2.06 s	1.05 m	0.48 m/s^2	8.96 m/s^2	NA	2.648	0.355
5283 (CIDM)	25.51 m/s	1.71 s	1.76 m	0.41 m/s^2	4.64 m/s^2	0.85	1.988	0.341

The calibration results employing RMSE(s) and RMSE(v) as objective functions are systematically presented in Table 1 and Table 2, respectively. These tables detail the calibrated parameters for each vehicle trajectory, along with the accompanying RMSE(s) and RMSE(v) values. Additionally, Figures 6 and 7 graphically compare the predicted speeds and gaps, respectively. A clear pattern emerges from both the tabular and graphical data: the performance in terms of RMSE(s) is lower when gap is used as the MoP, as opposed to when speed is used as MoP, and vice versa for RMSE(v). Notably, the magnitude of this discrepancy is significantly more pronounced when speed is employed as the MoP for calibration.

This observed discrepancy can be attributed to the following factors: When speed is the primary MoP, discrepancies in the model's predictions tend to accumulate over time and are further amplified. This is particularly evident in scenarios where the model's focus on minimizing velocity error (RMSE(v)) leads to an oversight in the accuracy of vehicle positioning. In this context, the model exhibits a 'memoryless' behavior with regard to spacing errors, suggesting a potential lack of adjustment in its parameters in response to spacing discrepancies over time. Conversely, when the calibration centers around minimizing RMSE(s), the model demonstrates increased sensitivity to vehicle positioning and spacing accuracy. This results in consistent adjustments of the model's parameters to ensure that the predicted spacing closely aligns with the observed data. The trade-off here is a marginal increase in velocity error, but this contributes to a more accurate prediction of spacing over time. On the other hand, the braking term $(\frac{s^*(v_n,\Delta v_n)}{s_n})^2$ is derived based on the current gap and the desired gap, which is insensitive to speed. Thus, using the gap as the MoP is preferable when calibrating. The subsequent analysis will be based on the results shown in Table 1.

In this study, the calibrated value of v_0 is not discussed because, the dataset does not contain the free flow scenario, and v_0 is calibrated from the free flow regime. On the other hand, the magnitude of the v_0 does not show a significant influence on predicting performance (*26*). Drawing a conclusion from the categorized analysis of the calibration results, it is reasonable to assert that the CIDM is generally a preferable choice over the IDM in various scenarios. This assertion is based on the following observations from the three categories:

CIDM Outperforms IDM: In several instances (vehicles 358, 730, and 5283), CIDM demonstrated superior performance compared to IDM, as indicated by lower RMSE(s) values, indicating a more precise simulation of car-following dynamics. For vehicle 358, Both models estimated similar parameters for a, T, and s_0. However, in the CIDM, a higher b value (2.50 m/s^2 compared to 1.28 m/s^2 in the IDM) and the incorporation of $R = 1.16$ correlated with a lower RMSE(s), suggesting that adjusting b alongside R potentially offers a more accurate reflection of driver behavior under certain conditions. This implies that the CIDM's framework, which accounts for driver sensitivity variations through R, can more accurately capture the dynamics of car-following behavior. For vehicle 730, all the estimated parameters in CIDM differ from those in IDM, with b increasing substantially to 6.13 m/s^2 from 0.18 m/s^2. The introduction of a high R value significantly reduces RMSE(s).For vehicle 5283, the CIDM's moderate adjustments in b and the introduction of $R = 2.91$ also resulted in a better model performance. These instances illustrate that the CIDM, with its additional parameter R, provides a valuable extension to the traditional IDM framework, enabling a more nuanced and flexible adaptation to varying driver sensitivities and behaviors.

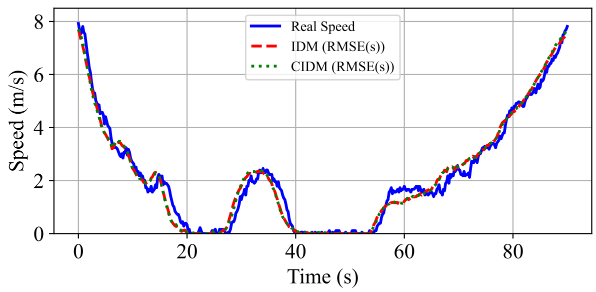

(a) Speed comparison for vehicle 358(RMSE(s))

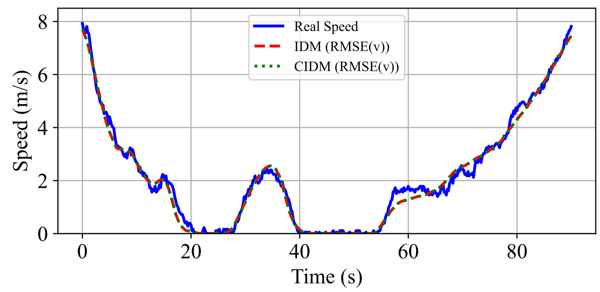

(b) Speed comparison for vehicle 358(RMSE(v))

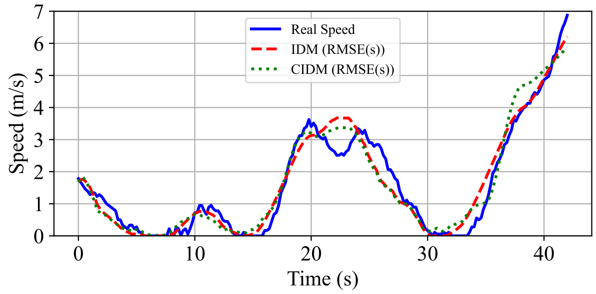

(c) Speed comparison for vehicle 730(RMSE(s))

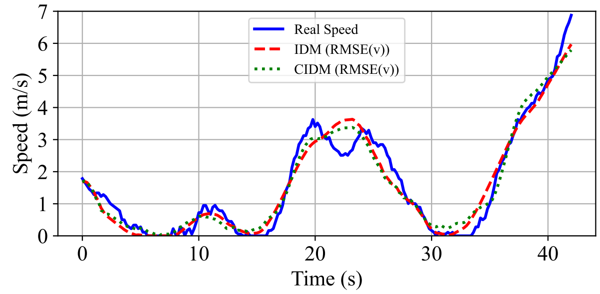

(d) Speed comparison for vehicle 730(RMSE(v))

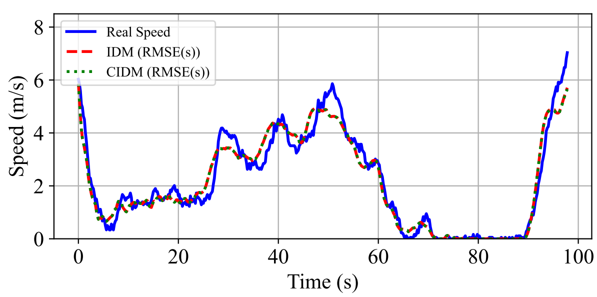

(e) Speed comparison for vehicle 1340(RMSE(s))

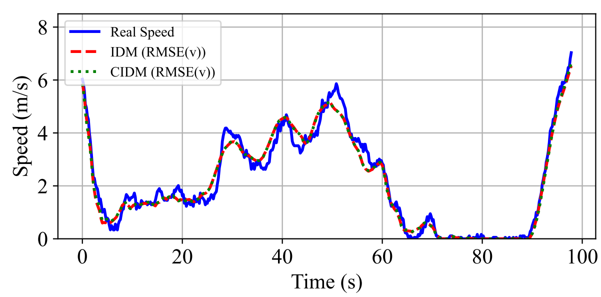

(f) Speed comparison for vehicle 1340(RMSE(v))

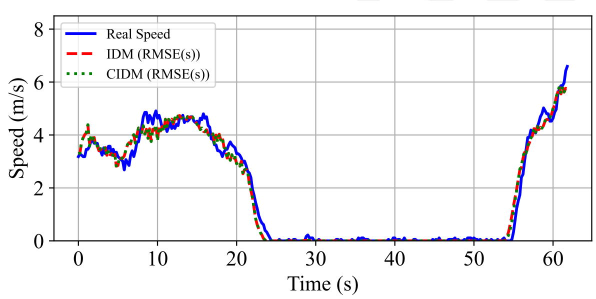

(g) Speed comparison for vehicle 1814(RMSE(s))

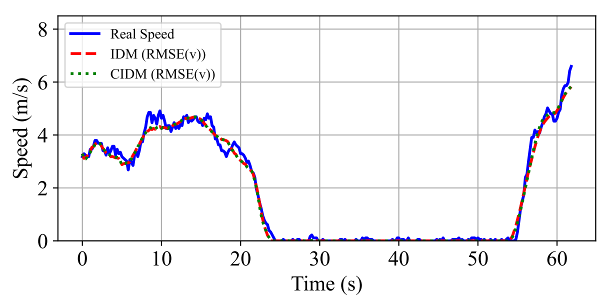

(h) Speed comparison for vehicle 1814(RMSE(v))

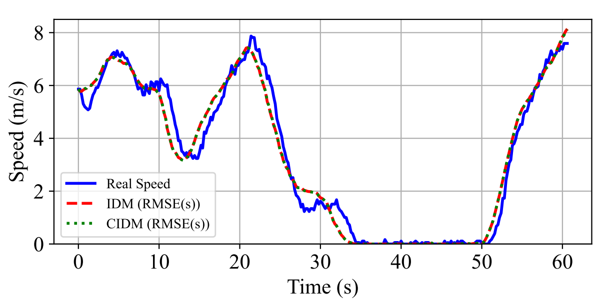

(i) Speed comparison for vehicle 4231(RMSE(s))

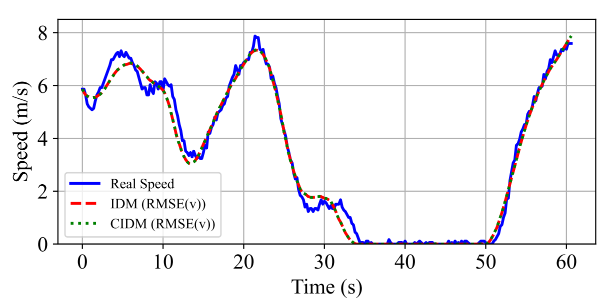

(j) Speed comparison for vehicle 4231(RMSE(v))

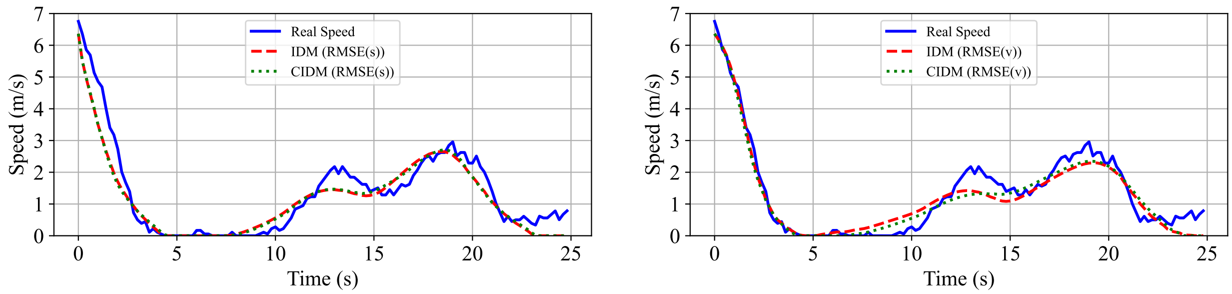

(k) Speed comparison for vehicle 5283(RMSE(s)) (l) Speed comparison for vehicle 5283(RMSE(v))

FIGURE 6: Comparison of estimated speed of IDM and CIDM using RMSE(s) and RMSE(v)

Similar Performance Between CIDM and IDM: In the case of vehicle 4231, CIDM and IDM exhibit nearly identical performance. In the CIDM, the estimated value of R is less than 0.1, suggesting that the conservative behavior typically enhanced by this parameter is not pronounced. Consequently, the other parameters estimated under the CIDM closely align with those derived from the IDM. This similarity implies that in scenarios where conservative driving behavior is minimally detected from the dataset, the CIDM adapts by mirroring the original IDM's parameters and performance. The fact that the CIDM neither underperformed nor significantly outperformed the IDM in this instance further validates its reliability and applicability in conditions similar to those modeled by traditional methods. This scenario underscores the CIDM's capability to operate equivalently to the IDM when the additional complexity introduced by R does not influence the driving behavior captured in the dataset.

Limitations Arising from Data Constraints: The calibration challenges encountered with vehicles 1340 and 1814, where both models hit the predefined limits of the b parameter, highlight significant data constraints rather than deficiencies within the models themselves. For vehicle 1814, although the CIDM estimates an R value of 3.39, resulting in a lower RMSE(s), the b values hit the lower threshold. Such calibration outcomes are deemed unsuccessful because a b value of 0.1 m/s^2 suggests extreme driver sensitivity, resulting in an unrealistic deceleration rate that is impractical for reliable simulations. Similarly, for vehicle 1340, the estimated b values in both models approach the upper limit of comfortable deceleration. As previously mentioned, neither exceedingly high nor low b values are appropriate for realistic simulations. Consequently, these instances of calibration are regarded as failures within this study, underscoring the challenges posed by insufficient data in accurately determining the comfortable deceleration term. This analysis suggests that the observed calibration failures stem not from inherent model flaws but from the limitations imposed by the available data.

In light of these findings, it can be concluded that CIDM is a viable and often superior alternative to IDM in various driving scenarios. Its ability to either outperform or match the performance of IDM, combined with the fact that the observed limitations are primarily due to data constraints, suggests that CIDM can be confidently utilized in diverse circumstances where accurate car-following behavior modeling is required. However, it is crucial to acknowledge that the effectiveness of CIDM, like any model, is contingent upon the availability and quality of the calibration data.

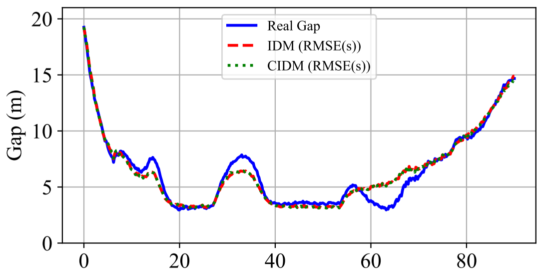

(a) Gap comparison for vehicle 358(RMSE(s))

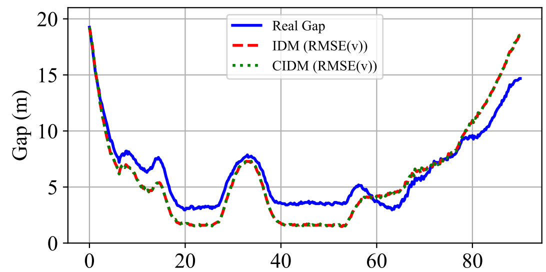

(b) Gap comparison for vehicle 358(RMSE(v))

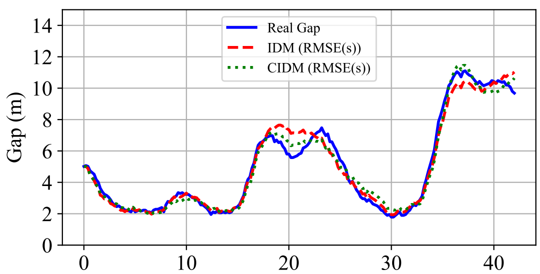

(c) Gap comparison for vehicle 730(RMSE(s))

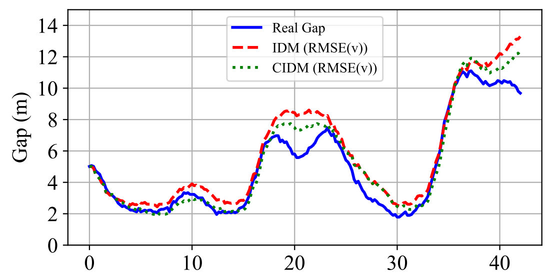

(d) Gap comparison for vehicle 730(RMSE(v))

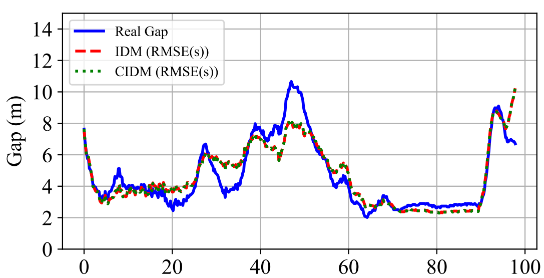

(e) Gap comparison for vehicle 1340(RMSE(s))

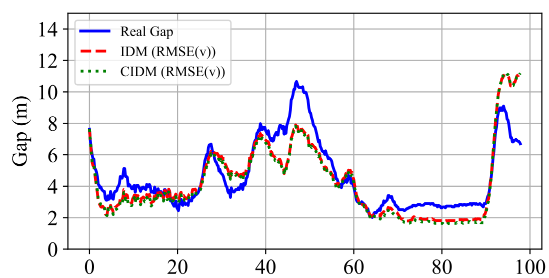

(f) Gap comparison for vehicle 1340(RMSE(v))

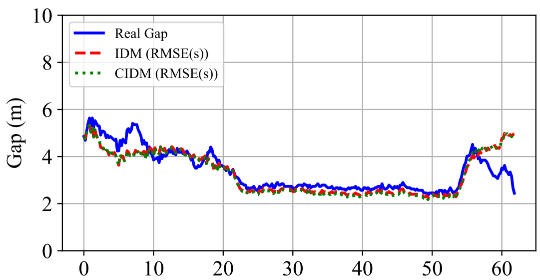

(g) Gap comparison for vehicle 1814(RMSE(s))

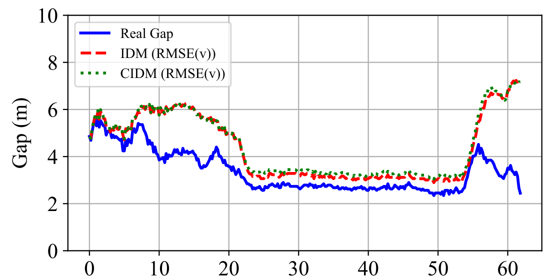

(h) Gap comparison for vehicle 1814(RMSE(v))

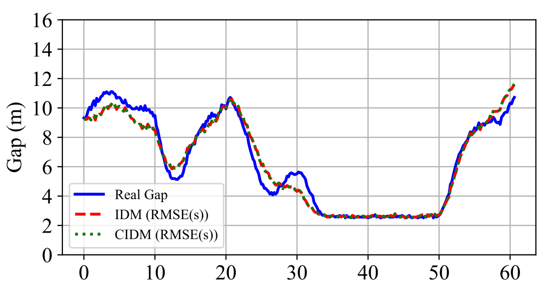

(i) Gap comparison for vehicle 4231(RMSE(s))

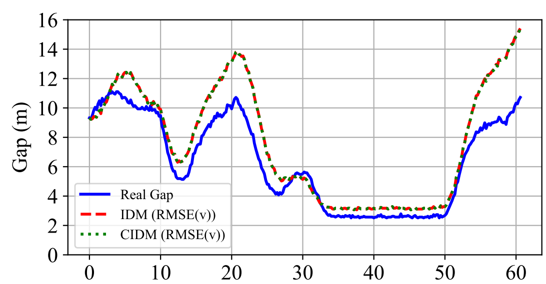

(j) Gap comparison for vehicle 4231(RMSE(v))

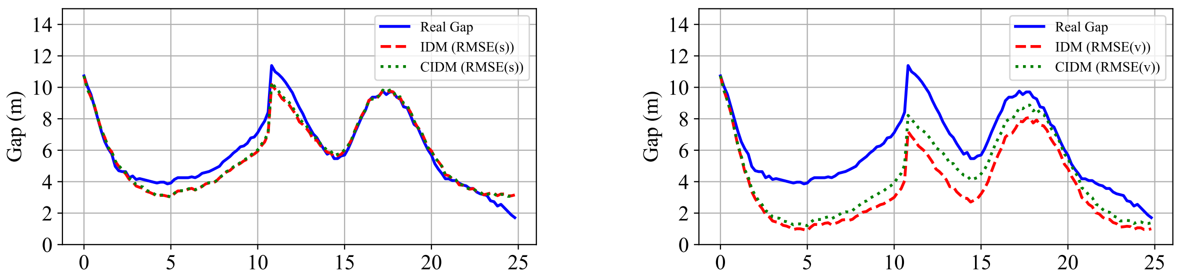

(k) Gap comparison for vehicle 5283(RMSE(s)) (l) Gap comparison for vehicle 5283(RMSE(v))

FIGURE 7: Comparison of estimated gap of IDM and CIDM using RMSE(s) and RMSE(v)

Case study 2: snowy weather conditions

The efficacy of the proposed model was further evaluated using a dataset collected under snowy weather conditions. Leveraging the approach established in the previous section, the combined MoP and GoF is determined using RMSE(s). The parameters for the GA execution remain consistent with the previous calibration process. Moreover, the boundary for the parameter b in both car-following models was the only adjustment made to accommodate the snowy weather conditions. Considering the increased severity of these conditions, it's unrealistic to expect drivers to adopt an aggressive braking strategy. Therefore, the boundary for b was specifically set at [0.1, 4] m/s^2, while the boundaries for all other parameters remained unchanged from the calibration for rainy weather conditions. The results of this calibration adjustment are documented in Table 3, and Figure 8 illustrates the simulation outcomes with these newly calibrated parameters.

The calibration results for various vehicles reveal insights into the performance of the CIDM compared to the traditional IDM. These findings can be categorized into three distinct groups, similar to patterns observed with datasets under rainy conditions. In the analysis of vehicles 269, 462, 659, and 727, the CIDM consistently outperformed the IDM, as indicated by lower RMSE(s) values across these cases. Specifically, for vehicle 269, the CIDM reduced RMSE(s) from 0.241 to 0.167 by slightly increasing the b parameter and introducing an R value of 3.12, which suggests a more nuanced adaptation to speed changes and improved stability. Vehicle 462 shows modest improvements with CIDM, where an increased b value and an R of 8.20 helped lower RMSE(s) from 0.568 to 0.548, indicating better compensation for abrupt driving maneuvers. In the case of vehicle 659, CIDM's adjustments resulted in a decrease in RMSE(s) from 0.131 to 0.125 by fine-tuning b and adding an R value of 1.70, which enhances the model's responsiveness to maintaining safer following distances. Most notably, vehicle 727 displayed significant improvement under CIDM, where RMSE(s) was substantially reduced from 0.147 to 0.121 through integrating an R of 8.18, thereby capturing the driver's deceleration behavior more accurately and effectively handling complex traffic dynamics. These results demonstrate CIDM's superior capability in simulating realistic car-following behaviors, particularly in dynamic and challenging driving environments, and highlight its potential in traffic modeling applications where traditional methods might not suffice.

These findings reinforce the CIDM's overall superiority in various driving scenarios, attributing its success to the model's capacity to integrate additional behavioral nuances through the R parameter. The performance disparities between the CIDM and IDM, particularly in cases where the CIDM demonstrates better fit and reduced error metrics, highlight the importance of incorporating broader behavioral factors into car-following models. Furthermore, the calibration challenges encountered, such as those with vehicle 221, accentuate the limitations of relying solely on traditional modeling approaches. Consequently, these results advocate for the adoption of the CIDM in efforts to achieve a more comprehensive and accurate simulation of driver behavior under diverse conditions.

TABLE 3: Calibration Results of IDM and CIDM with RMSE(s) of snowy dataset

Vehicle	v_0	T	s_0	a	b	R	RMSE(s)
123 (IDM)	14.91 m/s	0.86 s	4.85 m	2.17 m/s^2	3.62 m/s^2	NA	0.221
123 (CIDM)	14.92 m/s	0.87 s	4.84 m	2.14 m/s^2	3.23 m/s^2	0.02	0.222
221 (IDM)	19.31 m/s	2.36 s	2.91 m	0.35 m/s^2	0.10 m/s^2	NA	0.093
221 (CIDM)	21.56 m/s	2.28 s	4.56 m	3.79 m/s^2	2.53 m/s^2	7.69	0.043
269 (IDM)	13.29 m/s	1.64 s	1.17 m	2.35 m/s^2	3.76 m/s^2	NA	0.241
269 (CIDM)	13.15 m/s	1.56 s	1.07 m	2.04 m/s^2	3.95 m/s^2	3.12	0.167
462 (IDM)	32.49 m/s	0.44 s	4.98 m	3.92 m/s^2	0.97 m/s^2	NA	0.568
462 (CIDM)	30.94 m/s	0.47 s	4.99 m	2.71 m/s^2	2.71 m/s^2	8.20	0.548
659 (IDM)	12.56 m/s	2.03 s	2.14 m	3.14 m/s^2	3.72 m/s^2	NA	0.131
659 (CIDM)	13.37 m/s	2.07 s	2.49 m	3.98 m/s^2	3.92 m/s^2	1.70	0.125
727 (IDM)	31.50 m/s	1.62 s	3.49 m	0.96 m/s^2	3.94 m/s^2	NA	0.147
727 (CIDM)	26.41 m/s	1.47 s	3.24 m	0.94 m/s^2	3.54 m/s^2	8.18	0.121

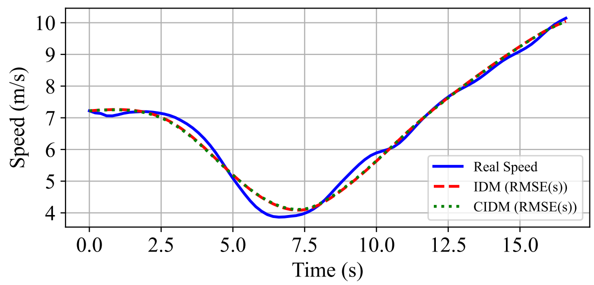

(a) Speed comparison for vehicle 123(RMSE(s))

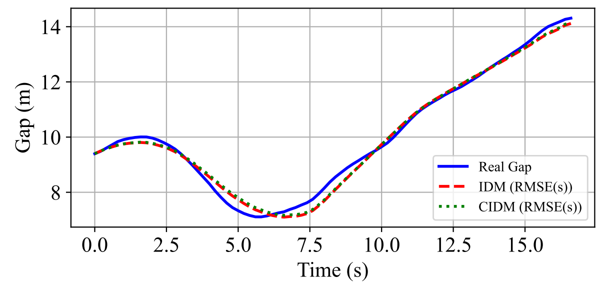

(b) Gap comparison for vehicle 123(RMSE(s))

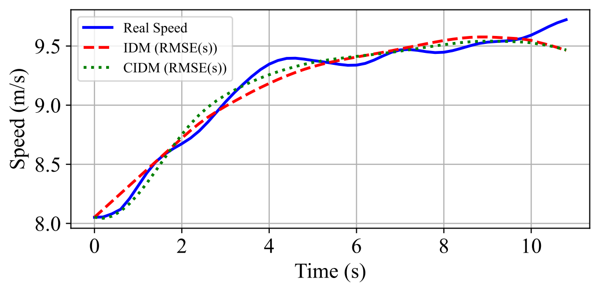

(c) Speed comparison for vehicle 221(RMSE(s))

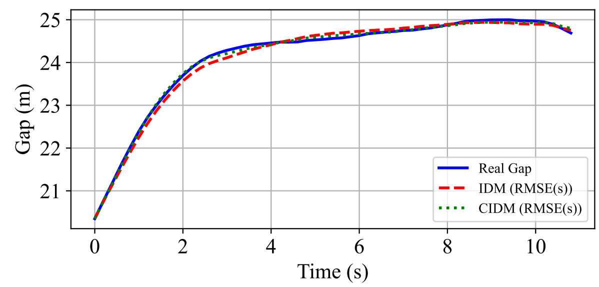

(d) Gap comparison for vehicle 221(RMSE(s))

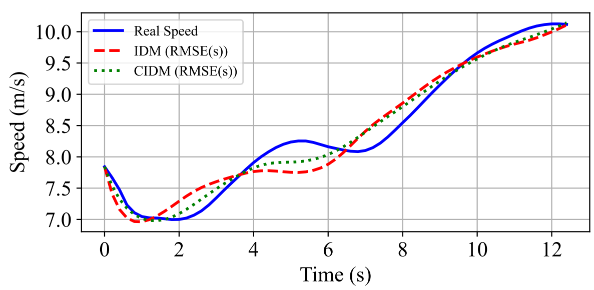

(e) Speed comparison for vehicle 269(RMSE(s))

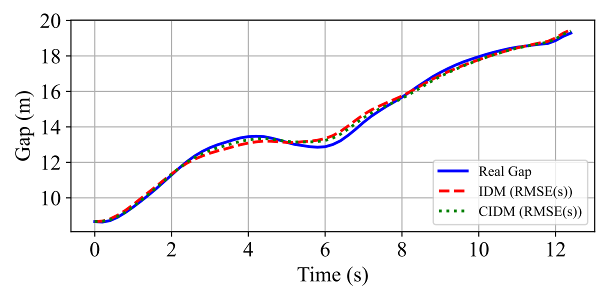

(f) Gap comparison for vehicle 269(RMSE(s))

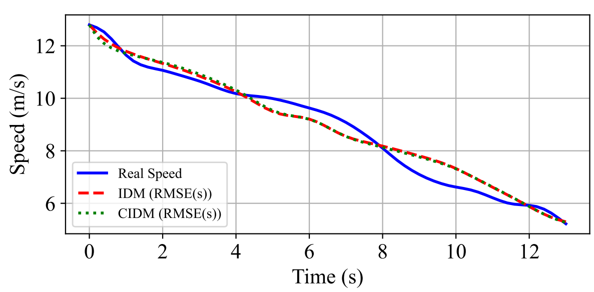

(g) Speed comparison for vehicle 462(RMSE(s))

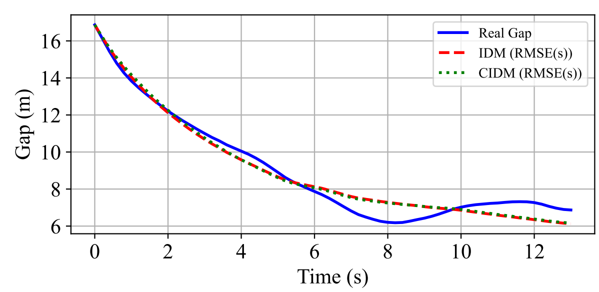

(h) Gap comparison for vehicle 462(RMSE(s))

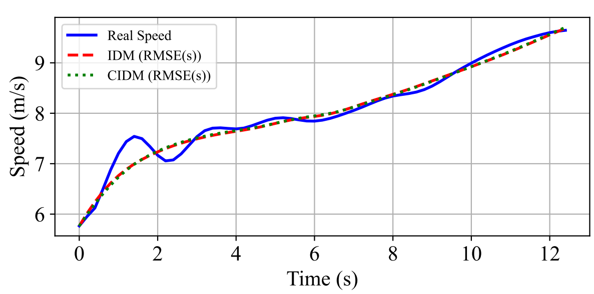

(i) Speed comparison for vehicle 659(RMSE(s))

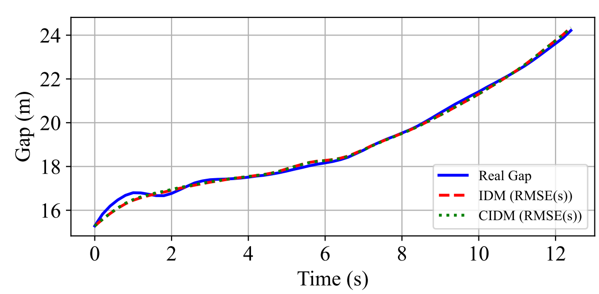

(j) Gap comparison for vehicle 659(RMSE(s))

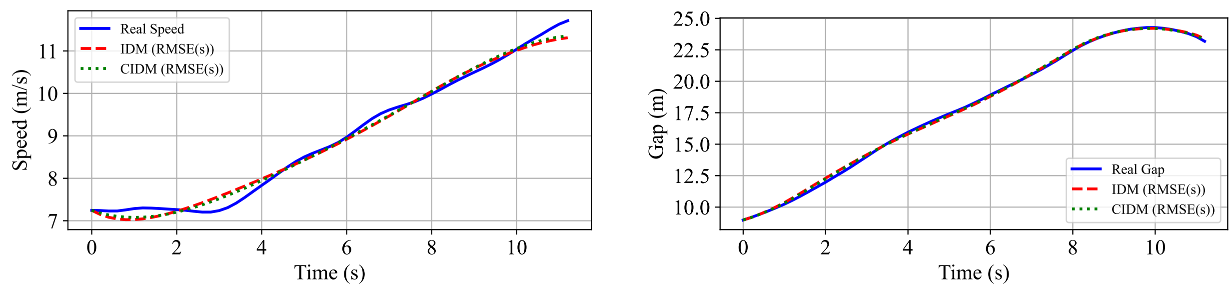

(k) Speed comparison for vehicle 727(RMSE(s)) (l) Gap comparison for vehicle 727(RMSE(s))

FIGURE 8: Results comparison of CIDM and IDM using snowy dataset

CONCLUSIONS

Car-following models are pivotal in analyzing traffic dynamics at the vehicle level. However, traditional car-following models often assume ideal environmental conditions, a scenario seldom encountered in reality, and frequently overlook the influence of weather on car-following behavior. This paper addresses such shortcomings by incorporating the impact of reduced visibility and road-tire friction into the car-following model. The IDM is employed as the base model due to its accurate simulations and clear physical interpretation of each parameter. The study initially examines the differences in driving behaviors under normal and adverse weather conditions and investigates the IDM's limitations in simulating such behaviors. Notably, to represent drivers' cautious braking behavior, the IDM often yields a smaller value for the comfortable deceleration rate, causing drivers to become oversensitive to critical conditions, potentially generating unrealistic deceleration rates. To mitigate this limitation, this study proposes the CIDM by introducing a single term to the IDM's desired gap function. This newly added term does not directly take changes in visibility and friction into consideration; instead, it attempts to capture the driver's cautious level in response to speed differences. Stability analysis has been conducted, and stability criteria have been derived. To further assess the proposed model's performance, real-world vehicle trajectories under rainy and snowy conditions were used for calibration. Two combinations of GoF and MoP are adopted for comparing the calibration results. The calibration results are classified into three groups: CIDM outperforms IDM, CIDM performs similarly to IDM, and both models fail due to data limitations. The results suggest that when conservative behavior is detectable from the dataset, the CIDM generates a lower estimated RMSE(s); when such behavior is not observed, the newly added term takes a negligible value and shows similar performance to the IDM. Therefore, it can be concluded that it is safe to calibrate the proposed model to simulate driving behavior under adverse weather conditions.

CREDIT

Kaitai Yang: Conceptualization, Methodology, Data collection and processing, Writing - original draft. **Yuan-Zheng Lei**: Conceptualization. **Yi Zhang**: Conceptualization, Data collection and processing. **Xianfeng Terry Yang**: Conceptualization, Methodology and Supervision.

ACKNOWLEDGEMENT

This research is supported by the award "OAC Core: Stochastic Simulation Platform for Assessing Safety Performance of Autonomous Vehicles in Winter Seasons (# 2234292)" which is funded by the National Science Foundation. The authors acknowledge the utilization of ChatGPT, a large language model, exclusively for enhancing the linguistic quality of the manuscript preparation process.

REFERENCES

1. May, A. D., *Traffic flow fundamentals*, 1990.
2. Chandler, R. E., R. Herman, and E. W. Montroll, Traffic dynamics: studies in car following. *Operations research*, Vol. 6, No. 2, 1958, pp. 165–184.
3. Gazis, D. C., R. Herman, and R. W. Rothery, Nonlinear follow-the-leader models of traffic flow. *Operations research*, Vol. 9, No. 4, 1961, pp. 545–567.
4. Han, J., X. Wang, and G. Wang, Modeling the car-following behavior with consideration of driver, vehicle, and environment factors: A historical review. *Sustainability*, Vol. 14, No. 13, 2022, p. 8179.
5. Gao, K., H. Tu, and H. Shi, Stage-specific impacts of hazy weather on car following. In *Proceedings of the Institution of Civil Engineers-Transport*, Thomas Telford Ltd, 2019, Vol. 172, pp. 347–359.
6. Zhang, W., C. Wang, Y. Shen, J. Liu, Z. Feng, K. Wang, and Q. Chen, Drivers' car-following behaviours in low-illumination conditions. *Ergonomics*, Vol. 64, No. 2, 2021, pp. 199–211.
7. Jiang, R. and Q.-S. Wu, The night driving behavior in a car-following model. *Physica A: statistical mechanics and its applications*, Vol. 375, No. 1, 2007, pp. 297–306.
8. Asamer, J., H. J. van Zuylen, and B. Heilmann, Calibrating car-following parameters for snowy road conditions in the microscopic traffic simulator vissim. *IET Intelligent Transport Systems*, Vol. 7, No. 1, 2013, pp. 114–121.
9. Park, S., H. Rakha, R. Alfelor, C. D. Yang, and D. Krechmer, Empirical study of impact of icy roadway surface condition on driver car-following behavior. *Transportation research record*, Vol. 2260, No. 1, 2011, pp. 140–151.
10. Saifuzzaman, M. and Z. Zheng, Incorporating human-factors in car-following models: a review of recent developments and research needs. *Transportation research part C: emerging technologies*, Vol. 48, 2014, pp. 379–403.
11. Treiber, M. and A. Kesting, Traffic flow dynamics. *Traffic Flow Dynamics: Data, Models and Simulation, Springer-Verlag Berlin Heidelberg*, 2013, pp. 983–1000.
12. Treiber, M., A. Kesting, and D. Helbing, Delays, inaccuracies and anticipation in microscopic traffic models. *Physica A: Statistical Mechanics and its Applications*, Vol. 360, No. 1, 2006, pp. 71–88.
13. Hjelkrem, O. A. and E. O. Ryeng, Chosen risk level during car-following in adverse weather conditions. *Accident Analysis & Prevention*, Vol. 95, 2016, pp. 227–235.
14. Chen, C., L. Li, J. Hu, and C. Geng, Calibration of MITSIM and IDM car-following model based on NGSIM trajectory datasets. In *Proceedings of 2010 IEEE International Conference on Vehicular Electronics and Safety*, IEEE, 2010, pp. 48–53.
15. Chebrolu, N., T. Läbe, O. Vysotska, J. Behley, and C. Stachniss, Adaptive robust kernels for non-linear least squares problems. *IEEE Robotics and Automation Letters*, Vol. 6, No. 2, 2021, pp. 2240–2247.

16. Zheng, O., M. Abdel-Aty, L. Yue, A. Abdelraouf, Z. Wang, and N. Mahmoud, Citysim: A drone-based vehicle trajectory dataset for safety-oriented research and digital twins. *Transportation Research Record*, 2022, p. 03611981231185768.
17. Kesting, A. and M. Treiber, Calibrating car-following models by using trajectory data: Methodological study. *Transportation Research Record*, Vol. 2088, No. 1, 2008, pp. 148–156.
18. Punzo, V., B. Ciuffo, and M. Montanino, Can results of car-following model calibration based on trajectory data be trusted? *Transportation research record*, Vol. 2315, No. 1, 2012, pp. 11–24.
19. Punzo, V., Z. Zheng, and M. Montanino, About calibration of car-following dynamics of automated and human-driven vehicles: Methodology, guidelines and codes. *Transportation Research Part C: Emerging Technologies*, Vol. 128, 2021, p. 103165.
20. da Rocha, T. V., L. Leclercq, M. Montanino, C. Parzani, V. Punzo, B. Ciuffo, and D. Villegas, Does traffic-related calibration of car-following models provide accurate estimations of vehicle emissions? *Transportation research part D: Transport and Environment*, Vol. 34, 2015, pp. 267–280.
21. Ngoduy, D., S. Lee, M. Treiber, M. Keyvan-Ekbatani, and H. Vu, Langevin method for a continuous stochastic car-following model and its stability conditions. *Transportation Research Part C: Emerging Technologies*, Vol. 105, 2019, pp. 599–610.
22. Zhao, S. and K. Zhang, A distributionally robust stochastic optimization-based model predictive control with distributionally robust chance constraints for cooperative adaptive cruise control under uncertain traffic conditions. *Transportation Research Part B: Methodological*, Vol. 138, 2020, pp. 144–178.
23. Yu, S., X. Zhao, Z. Xu, and Z. Shi, An improved car-following model considering the immediately ahead car's velocity difference. *Physica A: Statistical Mechanics and Its Applications*, Vol. 461, 2016, pp. 446–455.
24. Park, M., Y. Kim, and H. Yeo, Development of an Asymmetric car-following model and simulation validation. *IEEE Transactions on Intelligent Transportation Systems*, Vol. 21, No. 8, 2019, pp. 3513–3524.
25. Rhoades, C., X. Wang, and Y. Ouyang, Calibration of nonlinear car-following laws for traffic oscillation prediction. *Transportation research part C: emerging technologies*, Vol. 69, 2016, pp. 328–342.
26. Treiber, M. and A. Kesting, Microscopic calibration and validation of car-following models–a systematic approach. *Procedia-Social and Behavioral Sciences*, Vol. 80, 2013, pp. 922–939.